25th ABCM International Congress of Mechanical Engineering
October 20-25, 2019, Uberlândia, MG, Brazil

# COBEM-2019-0300
# THERMAL ANALYSIS OF HEAT SINKS: AN ANALYTICAL APPROACH

**Lívia M. Corrêa**
**Daniel J. N. M. Chalhub**
Graduate Program of Mechanical Engineering (PPG-EM), Group for Studies and Environmental Simulations in Reservoirs (GESAR), Rio de Janeiro State University (UERJ), Rua Fonseca Teles, 121, 20940-903, Rio de Janeiro, RJ, Brazil
livcorrea@yahoo.com.br, daniel.chalhub@eng.uerj.br

***Abstract.*** *In this work, the thermal analysis of heat sinks is proposed using an analytical approach. The mathematical modeling is composed of a three-dimensional base and two-dimensional fins. The oncoming heat flux from a heated chip attached at the bottom of the base needs to be cooled to ensure its good performance and long service life. For this reason, fins coupled at the top of the base of the heat sink are responsible for increasing the heat transfer and cool the system. Also at the top of the base, the air is flowing between fins contributing to the temperature's reduction of the system. The Classical Integral Transform Technique is applied for solving the formulation of fins and the base. The results show the more fins attached to the base, the lower is the temperature of the base in the heat sink.*

***Keywords:*** *Thermal Analysis, Heat Sink, Classical Integral Transform Technique*

## 1. INTRODUCTION

The thermal management in Solid-State Electronics (SSE) has been one critical issue in the design of modern electronic devices. The size reduction and the need for a better and more efficient power dissipation have motivated several studies about the cooling of electronic components. Cost-effective modifications such as heat sinks are considered a key point to minimize SSE's temperature.

Heat sinks and, more specifically, their heat dissipation instigated several works about analysis and optimization of their fins and how to enhance it for minimum temperature, consequently avoiding over-heated SSE. The work of Teertstra *et al.* (2000) presented an analytical model to approach the average heat transfer rate for forced convection, air-cooled, plate-fin heat sinks. The work of Lehtinen (2005) analyzed both heat conduction and convection in fins applying well-known analytical and experimental results for convective heat transfer. The geometry of the fin was also studied for maximizing the heat transfer. The work of Azarkish *et al.* (2010) investigated the geometry of the longitudinal fins with variable cross-sectional area achieving its optimum fin profile using a genetic algorithm. On the other hand, Cuce and Cuce (2014) tested different rectangular fins configurations to produce the maximum heat loss in a specific volume and length of fin numerically exposed to convection and radiation heat transfer.

Some recent heat sink problems were analyzed using analytical and numerical methodologies. One can mention the research developed by Türkakar and Okutucu-Özyurt (2012) regarding a dimensional optimization of silicon heat sinks for located multiple heat sources by minimizing the thermal resistance at constant pumping power. Furthermore, the work from Singh *et al.* (2018) used the LaPlace transform technique to solve the temperature distribution of 1D fin with internal heat generation and periodic boundary condition. The work (Zaretabar *et al.*, 2018) presents a heat transfer numerical simulation of a heat sink installed on a square chip of a computer using the fourth-order Runge-Kutta method to solve the non-linear heat transfer equation. Another numerical research which was developed by Malek and Shabani (2018) simulates macro and microscope heat transfer utilizing different formulations for different scales. The used methodology is based on spectral methods, solving it numerically by spectral discretization and finite differences method. The microscope analysis uses the dual-phase lag formulation and for the macroscope problems, commercial software was used for the simulations.

The Classical Integral Transform Technique is a powerful analytical method based on the separation of variables method and is mainly applied in linear problems, (Chalhub *et al.*, 2014). Integral transforms have been previously applied to electronic problems. Dantas (1996), for example, applied the integral transform technique on an encapsulated microchip problem and obtained the solution considering different thermal conductivity layers over the chip thickness. More recently, Corrêa and Chalhub (2017) presented the solution of Solid-state Electronics with one heat generation on its domain and solved by Classical Integral Transform Technique. For dealing with heat sinks, previously, Corrêa and Chalhub (2018b) presented a heat sink analysis considering different values for the heat transfer coefficient depending on the position of the fins. Also, Pinheiro *et al.* (2018) proposed the application of the Integral Transforms for solving the conjugated

radiation-conduction in a finned-tube configuration problem.

In this work, a thermal analysis of heat sinks (HS), which dissipate the oncoming heat from a Solid State Electronic, is proposed using an analytical approach. The mathematical modeling is composed of a three-dimensional base and bi-dimensional fins. First, the Classical Integral Transform Technique is used for solving the fins formulation, in the function of the heat flux which arrives from the base, which is an unknown value. To obtain the final solution for the 3D base, the Classical Integral Transform Technique is also applied. For the base, however, two directions instead of one, as happened on the fins, need to be transformed. For this reason, it is necessary to have a double summation for the inversion term and, as a consequence, more terms were required for its full convergence. The achieved solution depends on the heat flux which leaves the base to the fin, which is an unknown value. After achieving the solutions for fins and base, they are coupled to find the value of the heat flux in the fin-base contact interface. Finally, fins and base solutions are calculated again applying the heat flux value. The results show an analysis of the proposed approach of the heat sink base's temperature with one, two and six equally spaced fins. This developed routine also includes the possibility of having non-equally spaced fins.

## 2. TWO-DIMENSIONAL PARALLEL PLATE FINS FORMULATION

The mathematical formulation for the heat transfer on the rectangular fins is given by the energy equation in steady state. The material is considered isotropic. Since the thickness of the fin is much smaller when compared to its height and width, a partial lumping approach is performed in the x-direction and the final formulation is two-dimensional. The convection heat flux is also considered both sides of the fin. The fin is connected to the base on its bottom surface, as indicated in Figure 2. For this reason, the lower boundary is the contact interface flux between fin-base, $\dot{q}''_{base}$, which varies on $y$-direction. Hence, insulation is considered on the upper end of the fin.

$$k\left(\frac{\partial^2 T(y,z)}{\partial z^2}+\frac{\partial^2 T(y,z)}{\partial y^2}\right)=\frac{2h(T-T_f)}{\Delta x} \quad \text{for} \quad 0\le y\le W \quad \text{and} \quad 0\le z\le H_a \tag{1a}$$

$$-k\left.\frac{\partial T}{\partial z}\right|_{z=0}=\dot{q}''_{base}(y); \quad \left.\frac{\partial T}{\partial z}\right|_{z=H_a}=0; \quad \left.\frac{\partial T}{\partial y}\right|_{y=0}=0; \quad \left.\frac{\partial T}{\partial y}\right|_{y=W}=0 \tag{1b}$$

where $T$ is the temperature in $^o$C, $k$ is the thermal conductivity of the fin in W/(m.K), $h$ is the convection heat transfer coefficient in W/(m$^2$.K), $T_f$ is the temperature of the surrounding air in $^o$C, $\dot{q}''_{base}$ is the contact interface flux between fin-base in W/m$^2$. $\Delta x$, $W$ and $H_a$ are the dimensions of the fin in $x$, $y$ and $z$ directions, respectively, in m.

The non-dimensionalization of the problem leads to the following mathematical formulation:

$$\frac{\partial^2\Theta}{\partial\zeta_a^2}+\gamma_a^2\frac{\partial^2\Theta}{\partial\eta^2}-(2\mathrm{Bi}_{H_a}\beta_a)\Theta=0 \quad \text{for} \quad 0\le\eta\le 1 \quad \text{and} \quad 0\le\zeta_a\le 1 \tag{2a}$$

$$\left.\frac{\partial\Theta}{\partial\zeta_a}\right|_{\zeta_a=0}=-A_1\dot{q}''_{base}(\eta); \quad \left.\frac{\partial\Theta}{\partial\zeta_a}\right|_{\zeta_a=1}=0; \quad \left.\frac{\partial\Theta}{\partial\eta}\right|_{\eta=0}=0; \quad \left.\frac{\partial\Theta}{\partial\eta}\right|_{\eta=1}=0 \tag{2b}$$

The non-dimensional groups are defined as:

$$\zeta_a=\frac{z}{H_a}; \quad \eta=\frac{y}{W}; \quad \Theta=\frac{T-T_f}{\Delta T}; \quad \beta_a=\frac{H_a}{\Delta x}; \quad \gamma_a=\frac{H_a}{W}; \quad \mathrm{Bi}_{H_a}=\frac{hH_a}{k}; \quad A_1=\frac{H_a}{k\Delta T} \tag{3}$$

where $\zeta_a$ and $\eta$ are the dimensionless versions of $z$ and $y$, $\Theta$ is the dimensionless temperature, $\beta_a$ and $\gamma_a$ are aspect ratios, $\mathrm{Bi}_a$ is the Biot number and $A_1$ is a value which combines the height of the fin, its thermal conductivity and the expected temperature range for the problem ($\Delta T$).

## 3. THREE-DIMENSIONAL HEAT SINK BASE FORMULATION

The base of the heat sink presents the same materials properties of the fin and a total contact between base and fin is considered. The energy equation on the steady-state was also used for the mathematical formulation for the base, dealing now with a three-dimensional heat conduction problem. The contact interface flux between base and fin is combined with the convection flux when there is a vacancy of fins and then applied as a boundary condition on the top of the base. The oncoming heat flux from the chip is described as the boundary condition on the bottom of the base of the HS and insulation is considered for the other boundaries, in this work.

Figure 1 describes the schematic problem, their dimensions, and heat fluxes positions. It can be noticed the presence of one fin that receives the fin-base flux in all the extension of its width and the increase of the surface contact area on the system is responsible for more efficient heat dissipation of the system. The vacancy of fins allows that air cools the remain parts of the top surface of the HS, indicated by the convection flux by light blue arrows. The oncoming heat flux from the heated chip, $\dot{q}''_o$, is indicated by the red square at the bottom surface of the base.

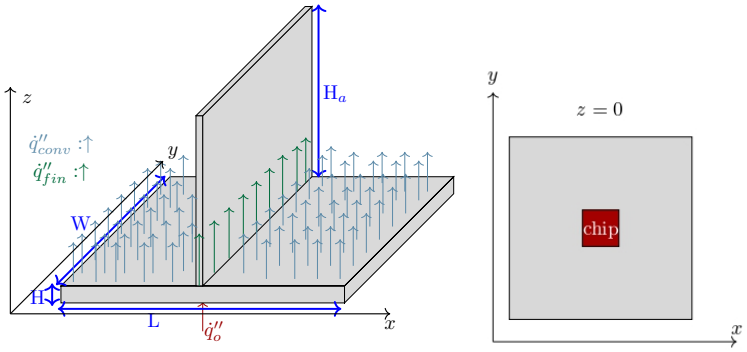


Figure 1: Heat sink front view.

The formulation for the base is shown below:

$$k\left(\frac{\partial^2 T}{\partial x^2}+\frac{\partial^2 T}{\partial y^2}+\frac{\partial^2 T}{\partial z^2}\right)=0 \quad \text{for} \quad 0\le x\le L, \quad 0\le y\le W \quad \text{and} \quad 0\le z\le H \tag{4a}$$

$$\left.\frac{\partial T}{\partial x}\right|_{x=0}=0; \quad \left.\frac{\partial T}{\partial x}\right|_{x=L}=0; \quad \left.\frac{\partial T}{\partial y}\right|_{y=0}=0; \quad \left.\frac{\partial T}{\partial y}\right|_{y=W}=0 \tag{4b}$$

$$-k\left.\frac{\partial T}{\partial z}\right|_{z=0}=\dot{q}''_o(x,y); \quad -k\left.\frac{\partial T}{\partial z}\right|_{z=H}=[\alpha(x)]\dot{q}''_{conv}+[1-\alpha(x)]\dot{q}''_{fin}(y) \tag{4c}$$

where $T$ is the temperature in $^o$C, $k$ is the thermal conductivity of the base in W/(m.K), $\dot{q}''_o$ is the oncoming flux from the heated chip, $\dot{q}''_{conv}$ is the convection flux at the top of the base and $\dot{q}''_{fin}$ is the contact interface flux between fin-base, all of them in W/m$^2$. $L$, $W$ and $H$ are the dimensions of the fin in $x$, $y$, and $z$ directions, respectively, in m. The parameter $\alpha$ is an embracing parameter to simplify the integral transform technique solution and defined as 0 or 1, indicates the position of the fins and the output flow present at a given position of $x$:

$$\alpha=\begin{cases}0 & \text{if the top is in contact with the fin, } (\dot{q}''_{fin}) \text{ is the boundary heat flux}\\ 1 & \text{if there is only convection in this position, } (\dot{q}''_{conv}) \text{ is the boundary heat flux}\end{cases} \tag{5}$$

The convection flux at the top of the base $\dot{q}''_{conv}$ is defined as:

$$\dot{q}''_{conv}=h(T-T_f) \tag{6}$$

where $h$ is the convection heat transfer coefficient in W/(m$^2$.K) and $T_f$ is the temperature of the surrounding air in $^o$C.

The non-dimensionalization of the problem leads to the following mathematical formulation:

$$\frac{\partial^2\Theta}{\partial\zeta^2}+\beta^2\frac{\partial^2\Theta}{\partial\eta^2}+\gamma^2\frac{\partial^2\Theta}{\partial\xi^2}=0 \quad \text{for} \quad 0\le\xi\le 1, \quad 0\le\eta\le 1 \quad \text{and} \quad 0\le\zeta\le 1 \tag{7a}$$

$$\left.\frac{\partial\Theta}{\partial\xi}\right|_{\xi=0}=0; \quad \left.\frac{\partial\Theta}{\partial\xi}\right|_{\xi=1}=0; \quad \left.\frac{\partial\Theta}{\partial\eta}\right|_{\eta=0}=0; \quad \left.\frac{\partial\Theta}{\partial\eta}\right|_{\eta=1}=0 \tag{7b}$$

$$\left.\frac{\partial\Theta}{\partial\zeta}\right|_{\zeta=0}=-A_2\dot{q}''_o(\xi,\eta); \quad \left.\frac{\partial\Theta}{\partial\zeta}\right|_{\zeta=1}=[-\alpha(\xi)]\mathrm{Bi}_H\Theta+[\alpha(\xi)-1]\,A_2\dot{q}''_{fin}(\eta) \tag{7c}$$

The non-dimensional groups are defined as:

$$\zeta=\frac{z}{H}; \quad \eta=\frac{y}{W}; \quad \xi=\frac{x}{L}; \quad \Theta=\frac{T-T_f}{\Delta T}; \quad \beta=\frac{H}{L}; \quad \gamma=\frac{H}{W}; \quad \mathrm{Bi}_H=\frac{hH}{k}; \quad A_2=\frac{H}{k\Delta T} \tag{8}$$

where $\zeta$, $\eta$ and $\xi$ are the dimensionless versions of $z$, $y$ and $x$, $\Theta$ is the dimensionless temperature, $\beta$ and $\gamma$ are aspect ratios, $\mathrm{Bi}_H$ is the Biot number and $A_2$ is a value which combines the height of the fin, its thermal conductivity and the range of temperature expected for the problem ($\Delta T$).

## 4. FIN-BASE COUPLING

Two assumptions are performed to couple the fin and base equations, which are considered having perfect contact. On the contact interface between fin and base, the temperature of the base at the top boundary and the position of the fin is the

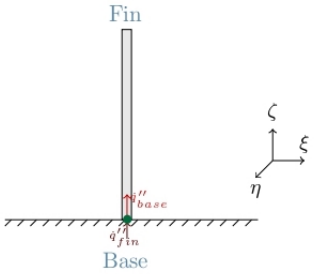


Figure 2: Fin-base coupling.

same temperature of the fin at the bottom boundary. This also happens to the heat fluxes, where the flux leaving the base on the position of the fin has the same intensity of the one which enters on the fin. Figure 2 shows a scheme in fin-base and the required conditions for the perfect interface contact, which are described below:

$$\dot{q}''_{base}(\eta) = \dot{q}''_{fin}(\eta) = \dot{q}''_{ic}(\eta) \tag{9}$$

$$\Theta_{base}(\text{position of the fin, prescripted value of } \eta, \text{ top of base}) = \Theta_{fin}(\text{prescripted value of } \eta, \text{ bottom of fin}) \tag{10}$$

Solving the equations separately so that $\dot{q}''_{base}$ and $\dot{q}''_{fin}$ are unknown values yet then, these mathematical equalities are performed and the value of $\dot{q}''_{base}$ and $\dot{q}''_{fin}$ are obtained. For this work, the heat fluxes may vary on $\eta$-direction and, for this reason, the heat fluxes $\dot{q}''_{base}$ and $\dot{q}''_{fin}$ are defined as:

$$\dot{q}''_{ic}(\eta) = \dot{q}''_{base}(\eta) = \dot{q}''_{fin}(\eta) = a_i\eta^3 + b_i\eta^2 + c_i\eta + d_i \tag{11}$$

where $a$, $b$, $c$ and $d$ are the coefficients for the heat flux and $i$ defines the fin which the heat flux belongs.

The fin and base equations are solved again replacing the unknown values for the new calculated values and finally, obtaining the temperature field for the coupled fin-base heat sink.

## 5. SOLUTION BY CLASSICAL INTEGRAL TRANSFORM TECHNIQUE

The analytical approach of this work will be achieved utilizing the Classical Integral Transform Technique. This is an analytical technique that uses expansions of the sought solution in terms of an infinite orthogonal basis of eigenfunctions, keeping the solution process always within a continuous domain. Because we are dealing with a 2D fin and a three-dimensional base, the inversion term would have a single summation for the fin while a double summation would be necessary for the base. The single and double summation had been already discussed and compared in (Chalhub *et al.*, 2014) and (Corrêa and Chalhub, 2018a), and for both previous works, it was concluded that the double requires more terms for the full convergence. The methodology of each part of the heat sink is described below.

### 5.1 CITT Solution for fin

To obtain the solution for the fin, the Classical Integral Transform Technique (CITT) is applied. As a precondition to establishing the transformation pair, the temperature field is written as a function of orthogonal eigenfunctions obtained from the following auxiliary eigenvalue problem known as the Helmholtz classic problem in cartesian coordinates. The eigenvalue problem proposed to be solved on the fin is in the $\eta$ direction, where $\Psi(\eta)$ are the eigenfunctions and $\lambda_n$ are the eigenvalues. For this particular problem, the case where $\lambda = 0$ also exists.

$$\Psi''_n(\eta) + \lambda_n^2\Psi_n(\eta) = 0 \tag{12a}$$

$$\Psi'_n(0) = 0, \quad \Psi'_n(1) = 0 \tag{12b}$$

Solving the differential equation, the solution shows that the eigenfunction is formed by sines and cosines. Applying the boundary conditions, the term formed by sines is eliminated from the solution and the values of the eigenvalues $\lambda_n$ are found.

For $\lambda = 0$ , the solution of the eigenvalue problem is given by:

$$\Psi_0(\eta) = 1; \qquad \lambda_0 = 0 \tag{13}$$

and for $\lambda > 0$ :

$$\Psi_n(\eta) = \cos(\lambda_n\eta); \qquad \lambda_n = n\pi, \quad \text{for} \quad n = 1, 2, 3, \ldots \tag{14}$$

The transformation pair for the fin is defined as:

$$\text{Transformation} \quad \Rightarrow \quad \bar{\Theta}_n(\zeta) = \int_0^1 \Theta \Psi_n(\eta) \mathrm{d}\eta \tag{15}$$

$$\text{Inversion} \quad \Rightarrow \quad \Theta = \sum_{n=0}^{\infty} \frac{\bar{\Theta}_n(\zeta)\Psi_n(\eta)}{N_{y_n}} \tag{16}$$

where $N_{y_n}$ is the norm and is described in equation (32).

The equation (2a) is written again, multiplied by $\Psi_n$ and integrated into the domain for $\eta$. The objective in this step is to obtain the transformed equation by the replacement of the terms with the transformation input for the transformation term.

$$\int_0^1 \frac{\partial^2 \Theta}{\partial \zeta_a^2} \Psi_n \mathrm{d}\eta + \gamma_a \int_0^1 \frac{\partial^2 \Theta}{\partial \eta^2} \Psi_n \mathrm{d}\eta - 2\mathrm{Bi}_{H_a} \beta_a \int_0^1 \Theta \Psi_n \mathrm{d}\eta = 0 \tag{17}$$

Finally, the transformed equation is obtained:

- For $\lambda > 0$ :

$$\bar{\Theta_{a}}_n'' - (\gamma_a^2 \lambda_n^2 + 2\mathrm{Bi}_{H_a}\beta_a)\bar{\Theta}_n = 0 \tag{18}$$

The transformed boundary conditions are:

$$\bar{\Theta}_n'(0) = -A_1 \dot{q}_{base}''(\eta); \qquad \bar{\Theta}_n'(1) = 0 \tag{19}$$

- For $\lambda = 0$ :

$$\bar{\Theta_{a}}_0'' - (2\mathrm{Bi}_{H_a}\beta_a)\bar{\Theta}_0 = 0 \tag{20}$$

The transformed boundary conditions are:

$$\bar{\Theta}_0'(0) = -A_1 \dot{q}_{base}''(\eta); \qquad \bar{\Theta}_0'(1) = 0 \tag{21}$$

The transformed equation achieve an analytical solution, shown on equations (22) and (23):

$$\bar{\Theta}_n(\zeta_a) = \frac{A_1 e^{\zeta \mathrm{a}\left(-\sqrt{2\mathrm{Bi}\beta \mathrm{a} + \pi^2 \gamma \mathrm{a}^2 n^2}\right)} \left(e^{2\zeta \mathrm{a}\sqrt{2\mathrm{Bi}\beta \mathrm{a} + \pi^2 \gamma \mathrm{a}^2 n^2}} + e^{2\sqrt{2\mathrm{Bi}\beta \mathrm{a} + \pi^2 \gamma \mathrm{a}^2 n^2}}\right)}{\left(e^{2\sqrt{2\mathrm{Bi}\beta \mathrm{a} + \pi^2 \gamma \mathrm{a}^2 n^2}} - 1\right)\sqrt{2\mathrm{Bi}\beta \mathrm{a} + \pi^2 \gamma \mathrm{a}^2 n^2}} \times \int_0^1 \dot{q}_{base}''(\eta)\cos(n\pi\eta)\mathrm{d}\eta \tag{22}$$

$$\bar{\Theta}_0(\zeta_a) = \frac{A_1 e^{-\sqrt{2\mathrm{Bi}\beta \mathrm{a}}\zeta \mathrm{a}} \left(e^{2\sqrt{2\mathrm{Bi}\beta \mathrm{a}}\zeta \mathrm{a}} + e^{2\sqrt{2\mathrm{Bi}\beta \mathrm{a}}}\right)}{\sqrt{2\mathrm{Bi}\beta \mathrm{a}}\left(e^{2\sqrt{2\mathrm{Bi}\beta \mathrm{a}}} - 1\right)} \int_0^1 \dot{q}_{base}''(\eta)\mathrm{d}\eta \tag{23}$$

### 5.2 CITT Solution for the base

After solving the transformed equation for the fin depending on $\dot{q}_{base}''$, the solution using the Classical Integral Transform Technique for the base is developed. As it was mentioned before, the three-dimensional base must be transformed in two directions, which are $\eta$, presenting a similar eigenvalue problem as the fin, and $\xi$.

$$\Psi_n''(\eta) + \lambda_n^2 \Psi_n(\eta) = 0 \tag{24a}$$
$$\Psi_n'(0) = 0, \quad \Psi_n'(1) = 0 \tag{24b}$$

$$\Xi_m''(\xi) + \mu_m^2 \Xi_m(\xi) = 0 \tag{25a}$$
$$\Xi_m'(0) = 0, \quad \Xi_m'(1) = 0 \tag{25b}$$

The eigenfunctions $\Psi(\eta)$ and $\Xi(\xi)$ are solved. $\lambda_n$ are the eigenvalues of $\Psi(\eta)$ and $\mu_m$ are the eigenvalues of $\Xi(\xi)$.

For $\lambda > 0$ :

$$\Psi_n(\eta) = \cos(\lambda_n \eta); \qquad \lambda_n = n\pi, \quad \text{for} \quad n = 1, 2, 3, \ldots \tag{26}$$

For $\lambda = 0$ :

$$\Psi_0(\eta) = 1; \qquad \lambda_0 = 0 \tag{27}$$

For $\mu > 0$ :

$$\Xi_m(\xi) = \cos(\mu_m \xi); \qquad \mu_m = m\pi, \quad \text{for} \quad m = 1, 2, 3, \ldots \tag{28}$$

For $\mu = 0$ :

$$\Xi_0(\xi) = 1; \qquad \mu_0 = 0 \tag{29}$$

The transformation pair for the base is defined as:

$$\text{Transformation} \quad \Rightarrow \quad \bar{\bar{\Theta}}_{nm}(\zeta) = \int_0^1 \int_0^1 \Theta \Psi_n(\eta) \Xi_m(\xi) \mathrm{d}\eta \mathrm{d}\xi \tag{30}$$

$$\text{Inversion} \quad \Rightarrow \quad \Theta = \sum_{n=0}^{\infty} \sum_{m=0}^{\infty} \frac{\bar{\bar{\Theta}}_{nm}(\zeta) \Psi_n(\eta) \Xi_m(\xi)}{N_{y_n} N_{x_m}} \tag{31}$$

where $\bar{\bar{\Theta}}_{nm}$ is the transformed version of $\Theta$. $N_{y_n}$ and $N_{x_m}$ are the norms and are defined in (32).

$$N_{x_m} = \int_0^1 \Xi_m^2 \mathrm{d}\xi; \quad N_{y_n} = \int_0^1 \Psi_n^2 \mathrm{d}\eta \tag{32}$$

The equation (7a) is written again, multiplied by $\Psi_n$ and $\Xi_m$ and integrated in the domain for $\eta$ and $\xi$. The objective in this step is to obtain the transformed equation by the replacement of the terms with the transformation input for the transformation term.

$$\int_0^1 \int_0^1 \frac{\partial^2 \Theta}{\partial \zeta^2} \Psi_n \Xi_m \mathrm{d}\eta \mathrm{d}\xi + \beta^2 \int_0^1 \int_0^1 \frac{\partial^2 \Theta}{\partial \eta^2} \Psi_n \Xi_m \mathrm{d}\eta \mathrm{d}\xi + \gamma^2 \int_0^1 \int_0^1 \frac{\partial^2 \Theta}{\partial \xi^2} \Psi_n \Xi_m \mathrm{d}\eta \mathrm{d}\xi = 0 \tag{33}$$

For dealing with the transformed boundary condition at the top of the base, some simplifications are performed. The parameter $\alpha$, which was defined previously as an embracing parameter for the integral transform simplification, and the dependence on $\xi$ of $\alpha$ turns impracticable to obtain the transformed term. Consequently, $\alpha(\xi)$ is approximated to an average value $\alpha_{avg}$, described on Equation (34). This approximation was performed to simplify the obtaining of the analytical solution. The convection term is written considering an average value for $\alpha$, as shown below, becoming a constant value in all the domain of $\xi$, which values 1:

$$\alpha_{avg} = \int_0^1 \alpha(\xi) \mathrm{d}\xi \tag{34}$$

The convection term is written again, applying the $\alpha_{avg}$ :

$$-\int_0^1 \int_0^1 \alpha(\xi) \mathrm{Bi}_H \Theta(\xi, \eta, 1) \Xi_m(\xi) \Psi_n(\eta) \mathrm{d}\eta \mathrm{d}\xi = -\alpha_{avg} \mathrm{Bi}_H \int_0^1 \int_0^1 \Theta(\xi, \eta, 1) \Xi_m(\xi) \Psi_n(\eta) \mathrm{d}\eta \mathrm{d}\xi = \\ - \alpha_{avg}(\xi) \mathrm{Bi}_H \bar{\bar{\Theta}}_{nm} \tag{35}$$

The term which connects fin-base is rewritten substituting the $\alpha(\xi)$ for 0 at the regions where the fins are located.

$$A_2 \int_0^1 \int_0^1 (\alpha(\xi) - 1) \dot{q}''_{fin}(\eta) \Xi_m(\xi) \Psi_n(\eta) \mathrm{d}\eta \mathrm{d}\xi = -A_2 \sum_{j=1}^{\mathrm{n_{fin}}} \int_0^1 \int_{\xi_{i_j}}^{\xi_{f_j}} \dot{q}''_{fin}(\eta) \Xi_m(\xi) \Psi_n(\eta) \mathrm{d}\xi \mathrm{d}\eta \tag{36}$$

where $\mathrm{n_{fin}}$ is the number of fins, $\xi_i$ refers to the position where the fin begins and $\xi_f$ where it ends.

Convection and interface contact terms are reunited and the final top boundary condition which is used for solving the transformed equations is:

$$\bar{\bar{\Theta}}'(1) = -\alpha_{avg} \mathrm{Bi}_H \bar{\bar{\Theta}}(1) - A_2 \sum_{j=1}^{\mathrm{n_{fin}}} \int_0^1 \int_{\xi_{i_j}}^{\xi_{f_j}} \dot{q}''_{fin}(\eta) \Psi_n(\eta) \Xi_m(\xi) \mathrm{d}\xi \mathrm{d}\eta \tag{37}$$

Finally, the transformed equation is obtained for different values of the eigenvalues:

- For $\lambda > 0$ and $\mu > 0$ :

$$\bar{\bar{\Theta}}''_{nm} - (\beta^2\mu_m^2 + \gamma^2\lambda_n^2)\bar{\bar{\Theta}}_{nm} = 0 \tag{38}$$

The transformed boundary conditions are:

$$\bar{\bar{\Theta}}'_{nm}(0) = -A_2 \int_0^1 \int_0^1 \dot{q}''_o(\xi,\eta)\Xi_m(\xi)\Psi_n(\eta)\mathrm{d}\eta\mathrm{d}\xi; \tag{39}$$

$$\bar{\bar{\Theta}}'_{nm}(1) = -\alpha_{avg}\mathrm{Bi}_H\bar{\bar{\Theta}}_{nm}(1) - A_2\sum_{j=1}^{\mathrm{n_{fin}}}\int_0^1\int_{\xi_{i_j}}^{\xi_{f_j}} \dot{q}''_{fin}(\eta)\Psi_n(\eta)\Xi_m(\xi)\mathrm{d}\xi\mathrm{d}\eta \tag{40}$$

- For $\lambda > 0$ and $\mu = 0$ :

$$\bar{\bar{\Theta}}''_{n0} - (\gamma^2\lambda_n^2)\bar{\bar{\Theta}}_{n0} = 0 \tag{41}$$

The transformed boundary conditions are:

$$\bar{\bar{\Theta}}'_{n0}(0) = -A_2 \int_0^1 \int_0^1 \dot{q}''_o(\xi,\eta)\Psi_n(\eta)\mathrm{d}\eta\mathrm{d}\xi; \tag{42}$$

$$\bar{\bar{\Theta}}'_{n0}(1) = -\alpha_{avg}\mathrm{Bi}_H\bar{\bar{\Theta}}_{n0}(1) - A_2\sum_{j=1}^{\mathrm{n_{fin}}}\int_0^1\int_{\xi_{i_j}}^{\xi_{f_j}} \dot{q}''_{fin}(\eta)\Psi_n(\eta)\mathrm{d}\xi\mathrm{d}\eta \tag{43}$$

- For $\lambda = 0$ and $\mu > 0$:

$$\bar{\bar{\Theta}}''_{0m} - (\beta^2\mu_m^2)\bar{\bar{\Theta}}_{0m} = 0 \tag{44}$$

The transformed boundary conditions are:

$$\bar{\bar{\Theta}}'_{0m}(0) = -A_2 \int_0^1 \int_0^1 \dot{q}''_o(\xi,\eta)\Xi_m(\xi)\mathrm{d}\eta\mathrm{d}\xi; \tag{45}$$

$$\bar{\bar{\Theta}}'_{0m}(1) - \alpha_{avg}\mathrm{Bi}_H\bar{\bar{\Theta}}_{0m}(1) - A_2\sum_{j=1}^{\mathrm{n_{fin}}}\int_0^1\int_{\xi_{i_j}}^{\xi_{f_j}} \dot{q}''_{fin}(\eta)\Xi_m(\xi)\mathrm{d}\xi\mathrm{d}\eta \tag{46}$$

- For $\lambda = 0$ and $\mu = 0$:

$$\bar{\bar{\Theta}}''_{00} = 0 \tag{47}$$

The transformed boundary conditions are:

$$\bar{\bar{\Theta}}'_{00}(0) = -A_2 \int_0^1 \int_0^1 \dot{q}''_o(\xi,\eta)\mathrm{d}\eta\mathrm{d}\xi; \tag{48}$$

$$\bar{\bar{\Theta}}'_{00}(1) = -\alpha_{avg}\mathrm{Bi}_H\bar{\bar{\Theta}}_{00}(1) - A_2\sum_{j=1}^{\mathrm{n_{fin}}}\int_0^1\int_{\xi_{i_j}}^{\xi_{f_j}} \dot{q}''_{fin}(\eta)\mathrm{d}\xi\mathrm{d}\eta \tag{49}$$

After performing these modifications, it was achieved an analytical solution for each equation. To obtain the final temperature of the 3D-base, the inversion formula (31) is applied.

## 6. RESULTS

The problem was described, the parallel plate fins formulation and the solution methodology were explained. After achieving an analytical solution for base and fins formulations, the fin-base coupling was performed and the heat flux $\dot{q}''_{ic}$ was obtained. The heat flux was then applied on the base and fin solutions and now, in this section, the results are shown. For all the tested cases, it was considered a square chip, as shown in Figure 3, with a constant flux of 200000 W/m$^2$, $\beta$ and $\gamma$ value $0.25$ each. The values for the fins are $\mathrm{Bi}_{H_a}\beta_a = 3$ and $\gamma_a = 0.5$. $A_1$ and $A_2$ value $5 \times 10^{-6}$ and $2.5 \times 10^{-6}$, respectively.

For the first layout, it was tested a heat sink with one fin at the middle of the base with $0.1$ of length. It was considered $\mathrm{Bi}_H = 0.01$ and $\alpha_{avg} = 0.9$. The layout for this first case can be observed in Figure 4a, as well as the boundary condition

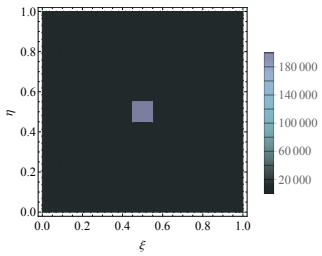


Figure 3: Chip coupled at the bottom of the base of HS and its heat flux.

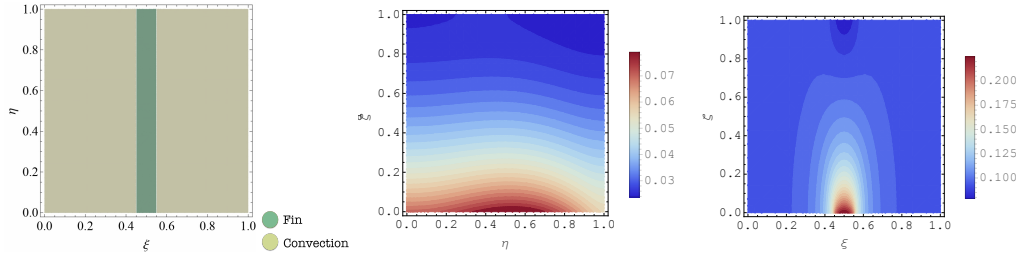


(a) Contour plot of the 1-fin Layout. (b) Solution for the fin. (c) Solution for $\mathrm{Bi}_H$=0.01 with $\eta$ fixed in 0.5.

Figure 4: Contour plot of the CITT solution for the 3D base$(\xi, \eta, \zeta)$ for the case with one fin and $\mathrm{Bi}_H$=0.01.

at the top of the base of the HS. The heat flux in the fin-base contact interface is indicated on equation (50) and the thermal profile of the fin is shown in Figure 4b.

$$\dot{q}''_{ic} = \dot{q}''_{base} = \dot{q}''_{fin} = 16386.6 - 8460.39\eta + 72522\eta^2 - 74769.4\eta^3 \tag{50}$$

It can be noticed a parabolic thermal profile for the 2D-fin, whose temperature achieve $0.0789451$ at the position (0.5,0), the same value at (0.5,0.5,0) on the 3D-base, which proves the assumption of the fin and base having the same temperature at their interface. At the position (0.5,1), the fin achieves $\Theta = 0.0252085$. The solution for the base is shown in Figure 4c, where isotherms curves bound the region where the chip is located in dark red, indicating warmer regions, and the position of the fin in dark blue for the regions with lower temperatures. It must be noticed the existence of ratio aspect in all the base Figures, for a better examination of the achieved results, the results are shown in a square plot. The base's hottest region is next to the chip's heat flux and the coolest region is near to the fin. Hence, it is important to be noticed the temperature field of the heat sink is not symmetric because of the non-symmetrical interface contact heat flux $\dot{q}''_{ic}$.

The second and third cases aim to evaluate how the increase of convection and fins enhance the cooling of the heat sink. The second case keeps $\alpha_{avg}$ and the layout of the first case and increases the value of $\mathrm{Bi}_H$ from $0.01$ to $0.1$ to evaluate how intense is the cooling of the system when the convection is intensified. The heat flux in the fin-base contact interface for this second case is indicated on equation (51) and, again, non-symmetrical interface contact heat fluxes caused not symmetric temperature field on the heat sink.

$$\dot{q}''_{ic} = 7487.2 - 8448.38\eta + 70929\eta^2 - 72980.2\eta^3 \tag{51}$$

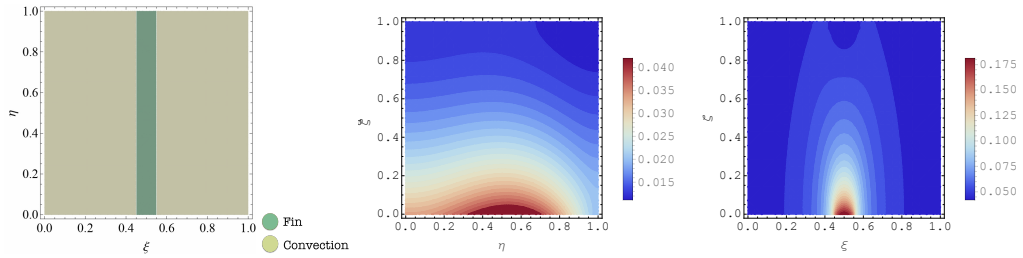


(a) Contour plot of the 1-fin Layout. (b) Solution for the fin. (c) Solution for $\mathrm{Bi}_H = 0.1$ with $\eta$ fixed in 0.5.

Figure 5: Contour plot of the CITT solution for the 3D base$(\xi, \eta, \zeta)$ for the case with one fin in the middle of the HS and $\mathrm{Bi}_H = 0.1$.

The enhance of convection on the heat sink promoted higher thermal dissipation and reduced the temperature field on the HS, in comparison with the first case. The temperature of the 2D-fin at (0.5,0), which was $0.0789451$, was reduced to

$0.0419756$ on this second case and at the top of the fin (0.5,1) was reduced to $0.0125758$ from $0.0252085$ of the previous case. However, if it is increased the number of fins in the HS, the thermal dissipation is passive and, consequently, more interesting to the industry.

The third case presents a different layout with 2 fins equally spaced from the middle of the base, shown in Figure 6a. It was considered $\mathrm{Bi}_H = 0.01$ and $\alpha_{avg} = 0.8$. Both fins presented similar non-symmetrical heat flux in the fin-base contact interface, indicated on equation (52):

$$\dot{q}''_{ic_1} = \dot{q}''_{ic_2} = 8585.24 - 743.681\eta + 24017.7\eta^2 - 27076.8\eta^3 \tag{52}$$

Because the fins present the same heat flux $\dot{q}''_{ic}$, the thermal profile is also the same, shown in Figure 6b. It can be noticed a relevant reduction on the fin temperature field in comparison with the first case tested (1 fin). This reduction in the temperature field is also noticed at the base. The temperature at the interface fin-base is $0.0415168$ for both fins. The thermal profile for the base is shown in Figure 6c, where the location of the fins is indicated by darker blue color isotherm region at the top of the base.

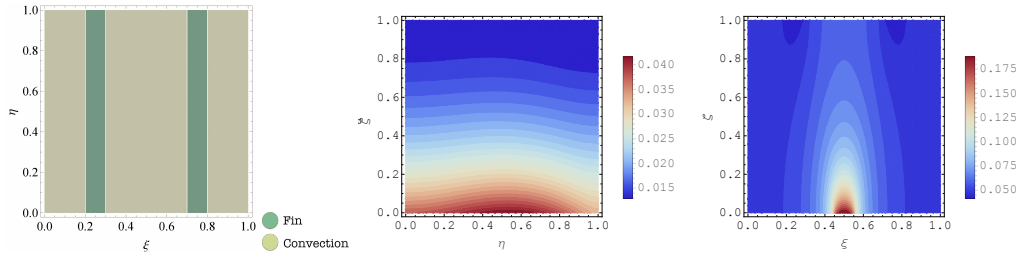


(a) Contour plot of the 2-fin Layout. (b) Solution for the fins. (c) Solution for $\mathrm{Bi}_H = 0.01$ with $\eta$ fixed in 0.5.

Figure 6: Contour plot of the CITT solution for the 3D base$(\xi, \eta, \zeta)$ for the case with two fins on the HS and $\mathrm{Bi}_H = 0.01$.

Analyzing Figures 5b and 5c for the second case and Figures 6b and 6c for the third case, it can be noticed the temperature ranges of the fin and base bounds the same intensity. In other words, despite different thermal profiles, the increase in Biot number promoted a similar thermal dissipation in comparison with the increase in the number of fins. However, it is more profitable to increase the number of fins, which promotes passive cooling, than enhance the heat transfer coefficient convection, which would require the use of a fan or other forced convection mechanisms. For this reason, the inclusion of fins in heat sinks is a more efficient cooling mechanism.

Finally, the final case proposes a layout with six finner fins, which is a layout more usual in the industry, shown in Figure 7a. It was considered $\mathrm{Bi}_H = 0.01$ and $\alpha_{avg} = 0.7$. The thermal profile for the third fin and base are shown in Figures 7b and 7c, respectively.

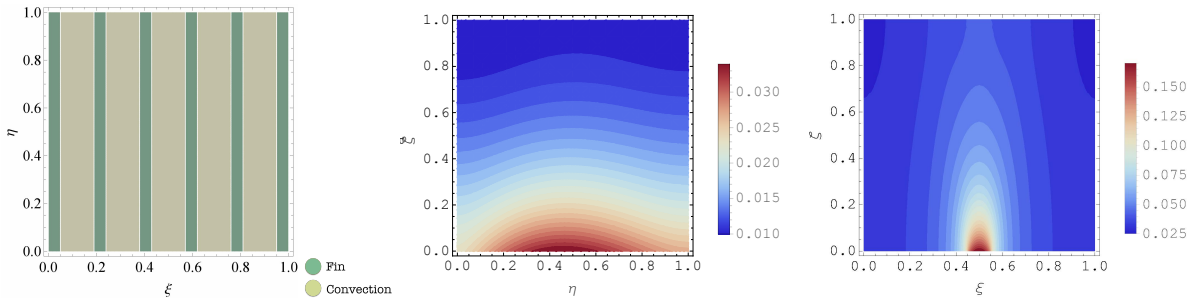


(a) Contour plot of the 6-fin Layout. (b) Solution for the third fin. (c) Solution for $\mathrm{Bi}_H = 0.01$ with $\eta$ fixed in 0.5.

Figure 7: Contour plot of the CITT solution for the 3D base$(\xi, \eta, \zeta)$ for the case with six fins on the HS and $\mathrm{Bi}_H = 0.01$.

The fact of having more fins distributed on the overall base, in fact, decreased the overall temperature of the base of the HS, contributing for a good performance of the heated chip, which keeps sending a heat flux to the bottom base at steady-state. In other words, the temperature along the heat sink had a sensitive reduce from the one-fin layout, which states that the efficiency of increasing fins to heat sinks to increase the heat dissipation and reduce the temperature.

## 7. CONCLUSION

This paper presented the thermal analysis of a heat sink dissipating heat from a solid-state electronic, solved utilizing the Classical Integral Transform Technique, which has shown to be a good alternative method for this kind of problem.

The parallel plate fins were described as two-dimensional and the base was formulated as three-dimensional. First, it was solved the formulation for the fin using the CITT single transformation. After obtained the analytical solution for the 2D-fin, the formulation for the 3D-base was solved using double transformations of the CITT and also achieved an analytical approach. Both solutions were coupled considering perfect contact assumptions and the interface contact heat flux between fin and base was found. Finally, this heat flux was applied to the fins and base solutions.

Different layouts of heat sinks, consequently, promote different heat fluxes between fin-base. The temperature field for both base and fins are not symmetric because of the non-symmetrical interface contact heat flux. The increase in the number of fins or convection enhances the heat dissipation on heat sinks. However, it was shown that is more profitable to add fins than enhance the heat transfer convection coefficient. Finally, the addition of fins performed the expected solution, which was the progressive reduction of the temperature as the number of fins increased. The six-fin layout was the most efficient for dissipating the oncoming heat flux and reducing the temperature.

## 8. ACKNOWLEDGEMENTS

The authors would like to acknowledge the financial support provided by CNPq, CAPES and FAPERJ, Brazilian agencies for the fostering of sciences.

## 9. REFERENCES

Azarkish, H., Sarvari, S.M.H. and Behzadmehr, A., 2010. "Optimum design of a longitudinal fin array with convection and radiation heat transfer using genetic algorithm". *International Journal of Thermal Sciences*, Vol. 49, pp. 2222–2229.

Chalhub, D.J.N.M., Sphaier, L.A. and de B Alves, L.S., 2014. "Semi-analytical method for the solution of the poisson equation derived from the navier-stokes using integral transform". In *ASME 2014 12th International Conference on Nanochannels, Microchannels and Minichannels collocated with the ASME 2014 4th Joint US-European Fluids Engineering Division Summer Meeting*. Chicago, Illinois, USA.

Corrêa, L.M. and Chalhub, D.J.N.M., 2017. "Solution of the heat conduction in solid-state electronics by integral transforms". In *24th ABCM International Congress of Mechanical Engineering - COBEM 2017*. Curitiba, Brazil.

Corrêa, L.M. and Chalhub, D.J.N.M., 2018a. "Comparison between single and double integral transformation of heat conduction in solid-state electronics". In *X Congresso Nacional de Engenharia Mecânica - CONEM 2018*. Salvador, Brazil.

Corrêa, L.M. and Chalhub, D.J.N.M., 2018b. "Thermal analysis of heat sink on solar panels". In *17th Brazilian Congress of Thermal Sciences and Engineering - ENCIT 2018*. Águas de Lindóia, Brazil.

Cuce, P.M. and Cuce, E., 2014. "Optimization of configurations to enhance heat transfer from a longitudinal fin exposed to natural convection and radiation". *International Journal of Low-Carbon Technologies*, Vol. 9, No. 4, pp. 305–310.

Dantas, L.B., 1996. *Estudo da Transferência de Calor por Encapsulamento Plástico Usando a Técnica da Transformada Integral Generalizada*. Master's thesis, Universidade Federal do Rio de Janeiro.

Lehtinen, A., 2005. *Analytical Treatment of Heat Sinks Cooled by Forced Convection*. Ph.D. thesis, Tampere University of Technology.

Malek, A. and Shabani, S.M.A., 2018. "Solving macroscopic and microscopic pin-fin heat sink problems by adapted spectral method". *Computational and Applied Mathematics*, Vol. 37, No. 2, pp. 1112–1129.

Pinheiro, I., Sphaier, L. and de B. Alves, L., 2018. "Integral transform solution of integro-differential equations in conduction-radiation problems". *Numerical Heat Transfer, Part A: Applications*, Vol. 73, No. Issue 2, pp. 94–114.

Singh, S., Kumar, D. and Rai, K., 2018. "Analytical solution of fourier and non-fourier heat transfer in longitudinal fin with internal heat generation and periodic boundary condition". *International Journal of Thermal Sciences*, Vol. 125, pp. 166–175.

Teertstra, P., Yovanovich, M.M. and Culham, J.R., 2000. "Analytical forced convection modeling of plate fin heat sinks". *Journal of Electronics Manufacturing*, Vol. 10, No. 4, pp. 253–261.

Türkakar, G. and Okutucu-Özyurt, T., 2012. "Dimensional optimization of microchannel heat sinks with multiple heat sources". *International Journal of Thermal Sciences*, Vol. 62, pp. 85–92.

Zaretabar, M., Asadian, H. and Ganji, D., 2018. "Numerical simulation of heat sink cooling in the mainboard chip of a computer with temperature dependent thermal conductivity". *Applied Thermal Engineering*, Vol. 130, pp. 1450–1459.

## 10. RESPONSIBILITY NOTICE

The authors are the only responsible for the printed material included in this paper.